Electrochimica Acta 56 (2011) 3115–3121

Contents lists available at ScienceDirect

Electrochimica Acta

journal homepage: www.elsevier.com/locate/electacta

Preparation and characterization of an $AuCu_3$ alloy electrode for electrocatalytic applications

Chun-Yen Tai[a], Jen-Lin Chang[a], Jyh-Fu Lee[b], Ting-Shan Chan[b], Jyh-Myng Zen[a,*]

[a] Department of Chemistry, National Chung Hsing University, 250 Kuo-Kuang Road, Taichung 402, Taiwan
[b] National Synchrotron Radiation Research Center, Hsinchu 300, Taiwan

ARTICLE INFO

Article history:
Received 9 November 2010
Received in revised form
20 December 2010
Accepted 19 January 2011
Available online 27 January 2011

Keywords:
Barrel plated electrode
$AuCu_3$
Alloy
Au electrode

ABSTRACT

We report here preparation and characterization of an $AuCu_3$ alloy electrochemical sensing platform fabricated on an easy for mass production barrel-plated gold electrode (AuBPE). Note that the AuBPE consists of Cu main body with successive plating of a very thin layer of Ni and Au (i.e., Cu–Ni–Au multilayer). By suitably manipulating the grain boundary diffusion between individual metallic layers of Cu–Ni–Au by means of thermal annealing treatment, $AuCu_3$ alloy film can be formed directly on the outer surface of the AuBPE. Electrochemical activation in alkaline solution can further generate a nanostructured $AuCu_3$ alloy film. This facile and novel approach is promising to prepare sensors for electroanalytical applications, e.g., glucose oxidation in pH-neutral solutions and simultaneous detection of uric acid, dopamine and ascorbic acid.

© 2011 Elsevier Ltd. All rights reserved.

1. Introduction

In recent years, our group has successfully applied the engineering process of barrel platting technology for mass production of a variety of metal electrodes in various analytical applications [1–5]. Among these, the barrel plated gold electrode (AuBPE) represents a useful platform for the development of a highly precise glucose biosensor [6–9]. The anodic current of the glucose biosensor is linked to the enzymatic reaction and varies linearly with the concentration of glucose in a certain range. Note that an accurate measurement of glucose level in blood has long been recognized as an important clinical test for diagnosing diabetes mellitus. We also successfully deposited a reticular and porous Ni film on the AuBPE to enhance the catalytic activity towards glucose oxidation [10]. The electro-oxidation of glucose, however, is only possible under alkaline conditions. In this study, we disclose a facile and novel approach to prepare $AuCu_3$ alloy film directly on the AuBPE and the as-prepared catalyst shows an interesting electrocatalytic oxidation of glucose in neutral media as well as other electrochemical sensing applications.

The main body of the AuBPE is made of Cu with successive plating of a very thin layer of Ni and Au (i.e., Cu–Ni–Au multilayer) and the Ni layer acts as a diffusion barrier to prevent any interactions between Cu and Au layers. Previous study on multilayer Cr–Cu–Ni–Au thin films indicated that the Ni layer is not effective as a diffusion barrier when annealing at 573 K for 900 s [11]. It is because that the high mixing energy of Au–Cu system can lead both Cu and Au diffuses towards each other across the Ni layer to exhibit intensive redistribution by the mechanism of grain boundary diffusion. Indeed, Au (r_{Au} = 0.1442 nm) and Cu (r_{Cu} = 0.1278 nm) with the radius difference is large, a complete statistical miscibility of Au and Cu in the solid phase is observed and can be described as solid solution [12,13]. Using the AuBPE with Cu–Ni–Au multilayer as a substrate, by suitably manipulating the grain boundary diffusion between individual metallic layers of Cu–Ni–Au, we demonstrate the formation of $AuCu_3$ alloy by a simple thermal annealing process. We further applied an electrochemical cyclic voltammetric activation process in alkaline solution to generate a nanostructured $AuCu_3$ alloy film. The XRD, XPS, SEM and AFM studies were executed to characterize the nanostructured $AuCu_3$ alloy and the results were discussed. Finally, the electrochemical sensing properties of the as-prepared nanostructured $AuCu_3$ alloy electrode were applied not only for electrocatalytic oxidation of glucose in neutral media but also for simultaneous determination of uric acid, dopamine and ascorbic acid.

2. Experimental

2.1. Measurements

All compounds were ACS-certified reagent grade and used without further purification. Aqueous solution was prepared with

* Corresponding author. Tel.: +886 4 22850864; fax: +886 4 22854007.
E-mail address: jmzen@dragon.nchu.edu.tw (J.-M. Zen).

0013-4686/$ – see front matter © 2011 Elsevier Ltd. All rights reserved.
doi:10.1016/j.electacta.2011.01.071

www.sgm.com.cn

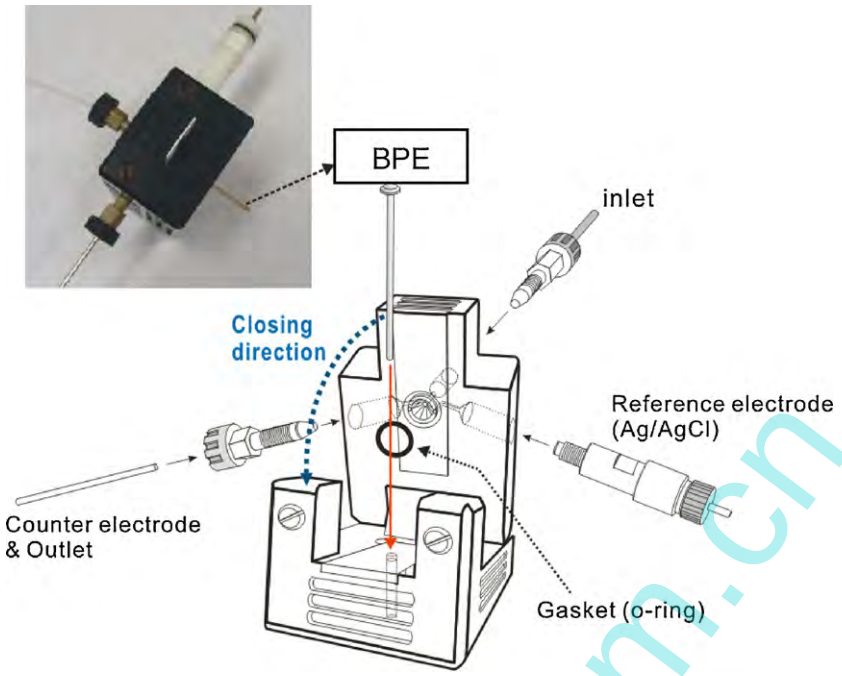

Fig. 1. Scheme and pictorial representation of the flow injection apparatus and the flow cell construction.

Millipore deionized water throughout this investigation. Cyclic voltammetric and chronoamperometric experiments were performed at a CHI 703 electrochemical workstation (CH Instruments, USA). Surface morphology of the film was examined with a field-emission scanning electron microscope (SEM, JEOL JSM-6700F) with an accelerating voltage of 3 kV. The thickness of Ni layer and Au layer was measured by X-ray fluorescence spectroscopy (FISCHERSCOPE® X-RAY XUL, FISCHER, Germany). The AFM images were recorded with a multimode scanning probe microscope system operated in tapping mode using Being Nano-Instruments CSPM-4000, Ben Yuan Ltd. (Beijing, China). Synchrotron XRD patterns were recorded with a large Debye–Scherrer camera installed at beam line 01C2 (λ = 1.033 Å or 12 keV) of National Synchrotron Radiation Research Center (NSRRC) in Taiwan. The flow injection analysis (FIA) system consisted of a high pressure microprocessor pump drive (BAS, USA) and a Rehodyne 7125 sample injection valve (20 μL loop) [3,5,10]. A flow cell (~50 μL of volume capacity), as shown in Fig. 1, was used for analytical measurements. It consists of an annealed-AuBPE working electrode, a stainless tube counter electrode (outlet), and an Ag/AgCl reference electrode. All the experiments were performed at room temperature (25 °C).

2.2. Electrode preparations

The AuBPE three-electrode system is the same as reported in our previous studies [6,10]. The AuBPE (1.25 mm diameter, 31 mm length) with an average weight of 392.4 ± 0.6 mg (n = 10) was fabricated by barrel plating nickel thin film onto a copper rod and subsequently plated gold thin film. The thickness of Ni layer and Au layer was measured as 7.39 μm and 0.11 μm, respectively. Note that the thickness of the outer Au layer can determine the rate and extent at which Ni should leach from the middle Ni layer. Also, the thickness of the Ni layer is important in the formation of the Au–Cu alloy since it would dictate the extent of interaction between Au and Cu layers. Annealing procedure was operated using a tube furnace. The AuBPE was annealed by a thermal step as follows: room temperature to 673 K for 40 min and then at 673 K for 2 h. The first low temperature annealing step can largely increase the grain boundary diffusion and the second high temperature step can help to form the miscible structure of $AuCu_3$. The optimum annealing conditions were selected according to its electrocatalytic performance to glucose oxidation. The annealed-AuBPE was activated by consecutive scanning in the range of −0.4 to 2.0 V for 150 segments in 0.1 M PBS (pH = 7) to leach out the Ni oxide component for generating of the nanostructured $AuCu_3$ film. Note that the activation conditions generally follow our previous studies [3,5,10]. Henceforth, the AuBPE prepared by thermal annealing followed by electrochemical treatment was designated as annealed-AuBPE and nanostructured-AuBPE, respectively.

3. Results and discussion

3.1. Structural characterizations

Fig. 2 shows the change in morphology of a bare AuBPE, the annealed-AuBPE and the nanostructured-AuBPE by SEM and AFM. As can be seen in the SEM pictures, compared to that of AuBPE, a grainy surface film was formed after the annealing process. Further electrochemical treatment was found to generate a nano-structure on the AuBPE. In effect, during the annealing procedure and electrochemical treatment, the appearance of AuBPE was observed to change from gold to brown and finally to chocolate, as illustrated in the inserted pictures. Both results of morphology and appearance change clearly indicate a variation of the outmost Au film after the thermal treatment.

Additional information regarding the variation in surface morphology of the AuBPE can be revealed by AFM studies. According to the AFM images, the smooth appearance of AuBPE was found to change into a relatively coarse and fracture surface after the annealing treatment. The electrochemical activation process further increased the rough level with the formation of nanosized pores on the surface. The change was clearly differentiated by the increase in surface contour level. Furthermore, based on the energy dispersive spectroscopy (EDS) analysis, the increase of Cu from 0.0 to 20.9 wt% accompanied with a decrease of Au from 69.3 to 48.8 wt% after the annealing process again indicates a possible Au

www.sjm.com.cn

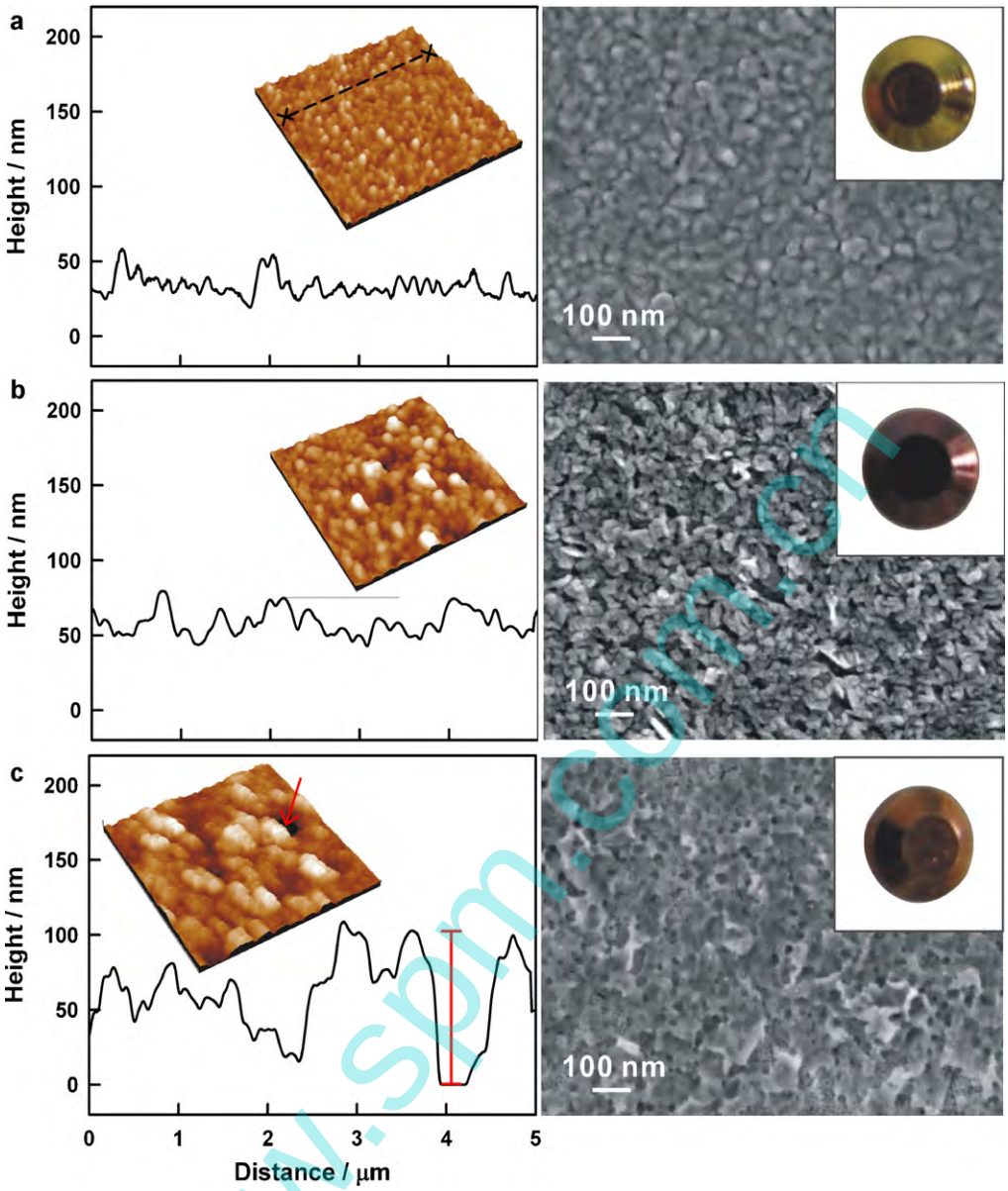

Fig. 2. AFM images, SEM images and pictures of AuBPE (a), annealed-AuBPE (b) and nanostructured-AuBPE (c), respectively.

alloy film formation. Overall, all these studies verified that there is indeed grain boundary diffusion between Au and Cu layers with a possible Au alloy formation. It is interesting that an Au–Cu alloy film can be achieved by a simple thermal annealing treatment followed by an electrochemical activation process.

We next aimed to study the two essential questions of: (1) what kind of Au alloy film is formed and (2) how the nanostructured film is attained? Fig. 3 shows the observed XRD patterns of a bare AuBPE, the annealed-AuBPE and the nanostructured-AuBPE, respectively. Due to the very thin thickness of Au layer, both the peaks responsible for the crystal reflections of Au and even the underneath Ni layer were observed at a bare AuBPE (i.e., before the annealing treatment, Fig. 3a). In accordance with the previous surface characterization studies, we observed new peaks corresponding to fundamental and superlattice reflections of $AuCu_3$ phase after the annealing treatment, as shown in Fig. 3b [12]. The original Ni layer underneath, on the other hand, was found to convert into Ni oxide during the annealing process. Note that the observation of very sharp diffraction peaks from the fundamental and superlattice reflections of $AuCu_3$ phase also reveals a homogeneous alloy structure after the annealing treatment. The relative ratio between the peaks related to $AuCu_3$ alloy and that of Ni oxide was found to increase after the electrochemical treatment with the re-appearance of a relatively smaller Au peak (Fig. 3c). We propose that it is the leaching of the Ni oxide component on the outer surface during the electrochemical activation process that generates the nano-structure and at the same time increases the relative ratio between $AuCu_3$ alloy and Ni oxide. Most importantly, the leaching of Ni oxide at the surface is essential to induce the electroactivity of the $AuCu_3$ alloy film as will be discussed in later section.

3.2. Electrochemical behavior

Cyclic voltammetric studies recorded before/after the annealing treatment and electrochemical activation process provide the most useful information regarding the application aspects. As shown in Fig. 4a, a typical Au redox peak (peaks a1/c1) at 0.81 V and 0.53 V was observed for the AuBPE before the annealing treatment. It is surprised that virtually no peak was observed in the voltammetric behavior of the annealed-AuBPE (Fig. 4b). During the

www.spm.com.cn

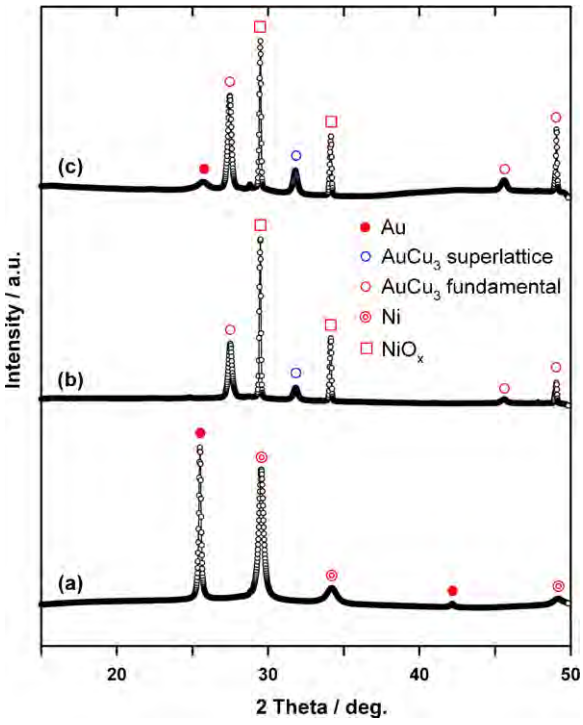

Fig. 3. XRD patterns for AuBPE (a), annealed-AuBPE (b) and nanostructured-AuBPE (c), respectively.

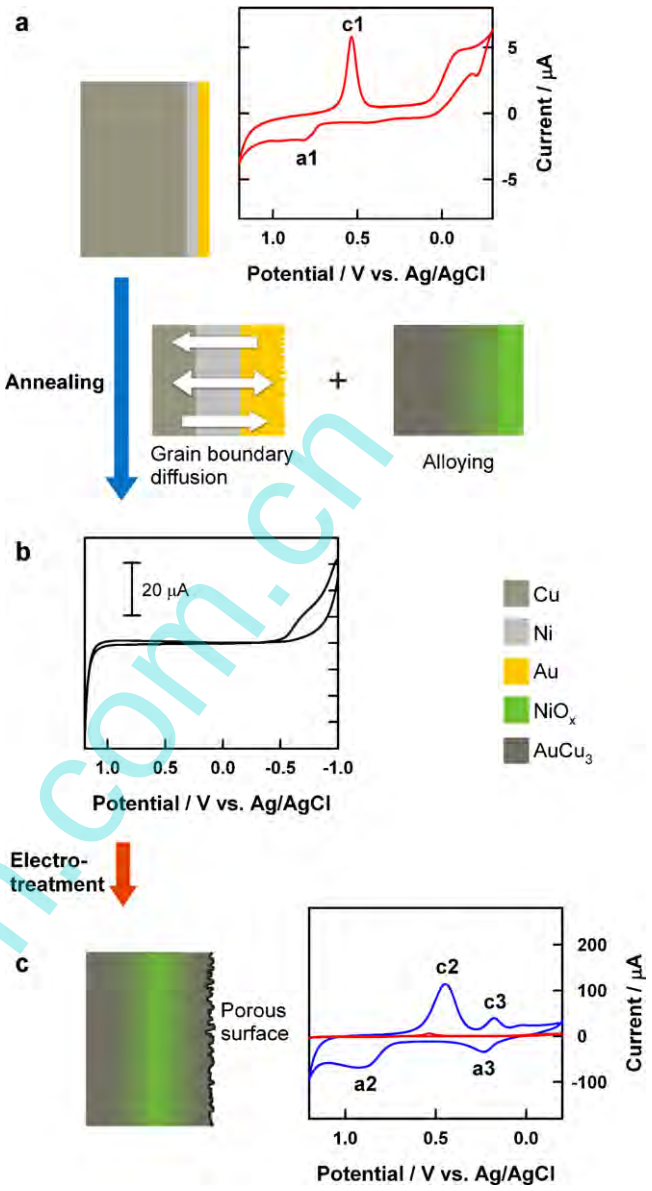

Fig. 4. Schematic of fabrication process with the observed cyclic voltammograms of AuBPE (a), annealed-AuBPE (b) and nanostructured-AuBPE (c, blue line) and AuBPE (red line) plotted together for comparison at a scan rate of 10 mV/s in 0.1 M PBS (pH = 7). (For interpretation of the references to color in this figure legend, the reader is referred to the web version of the article.)

electrochemical activation in pH 7 PBS, a couple of peaks (i.e., the redox peaks of a2/c2 at 0.96 V and 0.44 V and a3/c3 at 0.25 V and 0.18 V) were found to grow with successive cyclic voltammetric scanning (Fig. 4c). Most importantly, the much larger peak response of the nanostructured-AuBPE (blue line) to that of a bare AuBPE (red line) was in consistent with the SEM and AFM observations of which the nanostructured-AuBPE possesses a very high electroactive surface area. According to the disappearance/re-appearance of the Au signal in the XRD analysis before/after the electrochemical treatment, we believe that the peaks a2/c2 with a slightly shift in peak potentials to those of peaks a1/c1 is in fact the Au redox peak. The new peak a3/c3, on the other hand, should have something to do with the $AuCu_3$ redox peak.

Since the earlier XRD studies clearly verified the existence of Ni oxide after the annealing process and also the increase of relative ratio between $AuCu_3$ alloy and Ni oxide after electrochemical treatment. The existence of Ni oxide is thus critical to the lack of electroactivity for the annealed-AuBPE. Our previous investigation has demonstrated an activated Ni platform for electrochemical sensing of phosphate based on the adsorption of phosphate at the barrel plated nickel electrode (NiBPE) surface [5]. We suspect that the leaching of Ni oxide in the PBS medium may be the main driving force for such a phenomenon. As reported earlier, the electrochemical characteristics of the NiBPE is the loading effect of an oxidation peak at 0.53 V and a reduction peak at 0.38 V due to the activation of NiBPE in alkaline media to form a $Ni(OH)_2$/NiO(OH) film [13]. To check the cyclic voltammetric behavior of the annealed-AuBPE and nanostructured-AuBPE in alkaline solution can therefore provide the intrinsic information regarding Ni oxide. As shown in Fig. 5a, the multilayer formation phenomenon at the annealed-AuBPE was indeed similar to the electrochemical characteristics of the activated NiBPE. The cyclic voltammogram for the nanostructured-AuBPE, on the other hand, showed no such a loading effect corresponding to the characteristic peak of Ni oxide (Fig. 5b). We thus conclude that it is the Ni oxide that blocks the electroactivity of the $AuCu_3$ alloy film formed during the annealing process. The electrochemical activation that causes the leaching of the Ni oxide component is therefore essential for the occurrence of nano-structure as well as the electroactivity of the $AuCu_3$ alloy film.

3.3. Electrocatalytic activities

To evaluate the ability of the nanostructured-AuBPE for use in electrochemical sensing applications, nonenzymatic determination of glucose in neutral media was first demonstrated. Note that enzyme electrodes using glucose oxidase have been widely employed for the electro-oxidation of glucose, but with some drawbacks such as enzyme stability problems, interfering effects of other electrooxidizable species and the competing electron accepting reaction of O_2 with respect to the electrode [14–18]. Sensors based on the nonenzymatic direct oxidation of glucose would be expected to avoid such problems. Indeed, gold nanoparticles and gold nanos-

www.cpm.com.cn

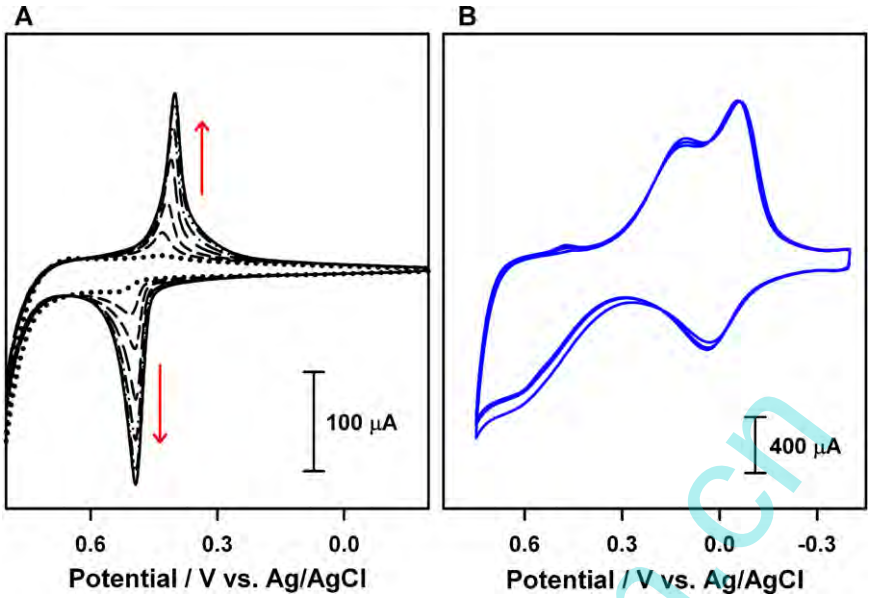

Fig. 5. (a) Cyclic voltammogram for consecutive 50 cycles at the annealed-AuBPE at a scan rate of 100 mV/s in 0.1 M NaOH solution. (b) The same experiments at the nanostructured-AuBPE.

tructured films modified electrodes have recently been introduced for the direct determination of glucose in neutral solutions [19–22]. Meanwhile, the conventional gold electrodes provided similar electroanalytical benefits after they were activated by cycling their potential between −0.20 V and 0.80 V [23]. The cyclization of electrode potential in PBS generates the gold–oxygen species on the electrode surface that catalyze the oxidation of glucose. In our case, the electrocatalytic behavior for glucose can be observable without activation. As shown in Fig. 6, there is an electrocatalytic peak for oxidation of glucose mediated by the a3/c3 redox couple at ~0.25 V vs. Ag/AgCl. The mediation of glucose by the $AuCu_3$ redox couple is thus confirmed in this study.

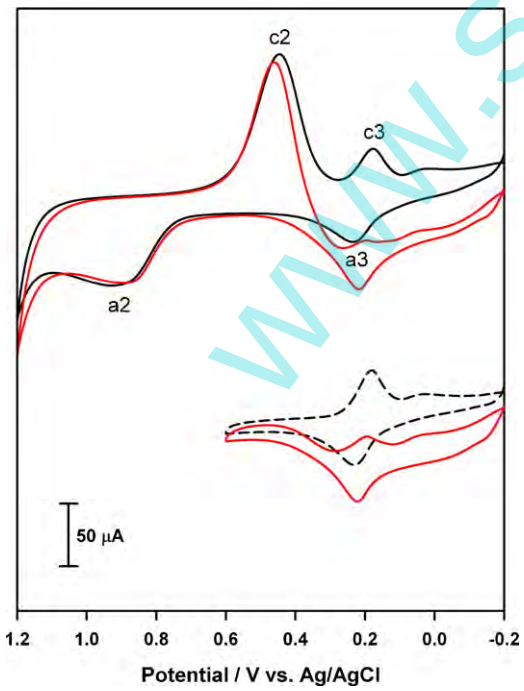

Fig. 6. Cyclic voltammograms of nanostructured-AuBPE at a scan rate of 10 mV/s in the absence (black line)/presence (red line) of 10 mM glucose in 0.1 M PBS (pH = 7). (For interpretation of the references to color in this figure legend, the reader is referred to the web version of the article.)

Compared to the chronoamperometric signals at a bare AuBPE, the nonenzymatic direct oxidation of glucose in neutral media is only possible at the nanostructured-AuBPE. At the detection potential of 0.25 V vs. Ag/AgCl, the amperometric responses of the nanostructured-AuBPE increased with successive additions of glucose. The excellent performance depicts the high electrocatalytic ability of the $AuCu_3$ alloy film not only with a large current enhancement but also with a largely decreased overpotential. Subsequently this characteristic of glucose at the nanostructured-AuBPE was employed for the detection of glucose by FIA. Note that important practical features of FIA include the simplicity, lower cost and better analytical characteristics. Besides, the instrumentation is lightweight, compact, easily be taken into the field and readily be automated. By taking 0.1 M, pH 7 PBS as the mobile phase, the mediated current of electrocatalytic oxidation of glucose at the nanostructured-AuBPE was utilized to electroanalysis of glucose. Fig. 7A shows typical FIA responses and calibration plot for glucose under the optimal conditions of H_f = 300 μL/min and E_{app} = 0.30 V vs. Ag/AgCl. A good linearity in the window of 20 μM to 10 mM with sensitivity of 1.75 μA/mM and regression coefficient of 0.999, respectively, was observed. The reproducibility of the proposed system was further checked by 10 continuous injections of 20 μM, 500 μM and 5 mM glucose (Fig. 7B). The relative standard deviations are 1.92%, 1.05% and 4.28% for 5 mM, 500 μM and 20 μM glucose, respectively. The fact that all relative standard deviations are <5% in the high to low concentrations of glucose indicates good reproducibility of the proposed system.

We further demonstrate simultaneous detection of uric acid, dopamine and ascorbic acid due to their importance in biological systems [24]. Simultaneous electrochemical detection of these three biomolecules is generally difficult at a bare carbon electrode because of the interference with one another. So far, many chemically modified electrodes including Au nanoparticles have been reported for this task [25–33]. Nonetheless, these modified electrodes generally are complicated and difficult to remain the stability. Fig. 8 compares the observed voltammetric responses for simultaneous detection of uric acid, dopamine and ascorbic acid at a bare AuBPE and the nanostructured-AuBPE. As can be

www.spm.com.cn

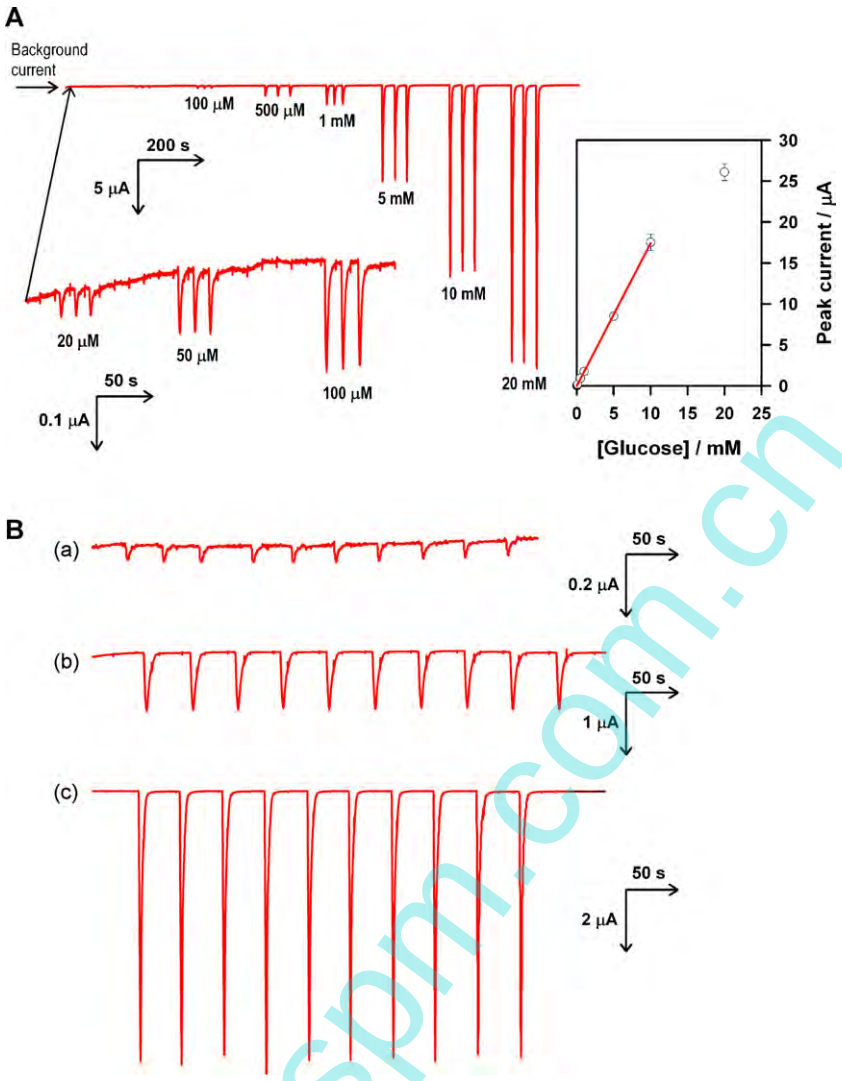

Fig. 7. (A) Typical FIA responses of glucose at a detecting potential of 0.3 V (vs. Ag/AgCl) and flow rate of 400 μL/min with 0.1 M PBS (pH = 7) carrier solution. (B) FIA responses of 20 μM (a), 500 μM (b) and 5 mM (c) glucose for 10 continuous injections.

seen, three distinguishable and much improved signals can only be observed at the nanostructured-AuBPE. Simultaneous detection of uric acid, dopamine and ascorbic acid without a separation step is thus promising using the nanostructured-AuBPE.

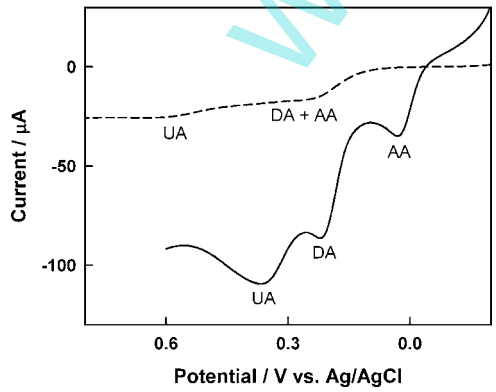

Fig. 8. Linear scan voltammograms at a bare AuBPE (dashed line) and the nanostructured-AuBPE (solid line) for 2 mM each of uric acid (UA), dopamine (DA), and ascorbic acid (AA) at a scan rate of 10 mV/s in 0.1 M PBS (pH = 7).

4. Conclusions

In conclusion, the $AuCu_3$ alloy film with nanosized pores have been prepared based on the AuBPE substrate by a simple thermal annealing procedure and electrochemical activation process. This facile approach is promising in manufacture on a mass scale and represents a useful platform for electroanalytical applications. We further demonstrated the application of the nanostructured-AuBPE for direct oxidation of glucose in neutral media with excellent electrocatalytic responses. The $AuCu_3$ alloy film is also an advanced material to catalyze the oxidation of uric acid, dopamine and ascorbic acid with improved voltammetric peak separation and sensitivity. Such an electrocatalytic property of the $AuCu_3$ alloy is anticipated to be used as anode in sugar–air battery with good energy densities [34–36]. The research is currently under investigation in this laboratory.

Acknowledgements

This work was supported by National Science Council of Taiwan and in part by the Ministry of education, Taiwan under the ATU plan and the boost program of NTHU.

www.spm.com.cn

References

[1] J.W. Sue, A.S. Kumar, H.H. Chung, J.M. Zen, Electroanalysis 17 (2005) 1245.
[2] J.W. Sue, C.Y. Tai, W.L. Cheng, J.M. Zen, Electrochem. Commun. 10 (2008) 277.
[3] J.W. Sue, C.J. Hung, W.J. Chen, J.M. Zen, Electroanalysis 20 (2008) 1647.
[4] Y. Shih, K.L. Wu, J.W. Sue, A.S. Kumar, J.M. Zen, J. Pharm. Biomed. Anal. 48 (2008) 1446.
[5] W.L. Cheng, J.W. Sue, W.C. Chang, J.L. Chang, J.M. Zen, Anal. Chem. 82 (2010) 1157.
[6] C.T. Hsu, H.H. Chung, D.M. Tsai, M.Y. Fang, H.C. Hsiao, J.M. Zen, Anal. Chem. 81 (2009) 515.
[7] C.T. Hsu, H.C. Hsiao, M.S. Lee, S.F. Chang, T.C. Lee, Y.S. Tsai, J.M. Zen, Clin. Chim. Acta 402 (2009) 119.
[8] M.H. Wu, M.Y. Fang, L.N. Jen, H.C. Hsiao, A. Muller, C.T. Hsu, Clin. Chem. 54 (2008) 1689.
[9] C.T. Hsu, H.C. Hsiao, M.Y. Fang, J.M. Zen, Biosen. Bioelectron. 25 (2009) 383.
[10] C.Y. Tai, J.L. Chang, J.M. Zen, Chem. Commun. (2009) 6083.
[11] M.I. Daylenko, M. Watanabe, C. Li, A.V. Krajnikov, D.B. Williams, M.A. Vasiliev, Thin Solid Films 444 (2003) 75.
[12] T.B. Massalski, H. Okamoto, P.R. Subramanian, L. Kacprzak, Binary Alloy Phase Diagrams, 2nd ed., ASM International, Metals Park, Ohio, 1991.
[13] S. Kameoka, A.P. Tsai, Catal. Lett. 121 (2008) 337.
[14] A. Heller, Acc. Chem. Res. 23 (1990) 128.
[15] S. Cho, C. Kang, Electroanalysis 19 (2007) 2315.
[16] A. Badia, R. Carlini, A. Fernandez, F. Battaglini, S.R. Mikkelsen, A.M. English, J. Am. Chem. Soc. 115 (1993) 7053.
[17] E. Bakker, Anal. Chem. 76 (2004) 3285.
[18] N. Mano, F. Mao, A. Heller, J. Am. Chem. Soc. 125 (2003) 6588.
[19] Y.G. Zhou, S. Yang, Q.Y. Qian, X.H. Xia, Electrochem. Commun. 11 (2009) 216.
[20] Y. Li, Y.Y. Song, C. Yang, X.H. Xia, Electrochem. Commun. 9 (2007) 981.
[21] H. Zhang, J.J. Xu, H.Y. Chen, J. Phys. Chem. C 112 (2008) 13886.
[22] W. Zhao, J.J. Xu, C.G. Shi, H.Y. Chen, Electrochem. Commun. 8 (2006) 773.
[23] M. Wooten, J.H. Shim, W. Gorski, Electroanalysis 22 (2010) 1275.
[24] G. Dryhurst, Electrochemistry of Biological Molecules, Academic Press, New York, 1977.
[25] G. Kang, X. Lin, Electroanalysis 18 (2006) 2458.
[26] K.S. Prasad, G. Muthuraman, J.M. Zen, Electrochem. Commun. 10 (2008) 559.
[27] J.L. Chang, K.H. Chang, C.C. Hu, W.L. Cheng, J.M. Zen, Electrochem. Commun. 12 (2010) 596.
[28] S. Shahrokhian, M. Ghalkhani, Electrochim. Acta 51 (2006) 2599.
[29] H. Yao, Y. Sun, X. Lin, Y. Tang, L. Huang, Electrochim. Acta 52 (2007) 6165.
[30] S. Shahrokhian, H.R. Zere-Mehurjardi, Electroanalysis 19 (2007) 2234.
[31] G. Hu, Y. Ma, Y. Guo, S. Shao, Electrochim. Acta 53 (2008) 6610.
[32] H. Liu, Y. Tian, Electroanalysis 20 (2008) 1227.
[33] P. Kannan, S.A. John, Anal. Biochem. 386 (2009) 65.
[34] V. Coman, C. Vaz-Domínguez, R. Ludwig, W. Herreither, D. Haltrich, A.L. De Lacey, T. Ruzgas, L. Gorton, S. Shleev, Phys. Chem. Chem. Phys. 10 (2008) 6093.
[35] Y. Yan, W. Zheng, L. Su, L. Mao, Adv. Mater. 18 (2006) 2639.
[36] G.W. Yang, C.L. Xu, H.L. Li, Chem. Commun. (2008) 6537.

www.spm.com.cn